Vol 13 No 9, September 2004
1009-1963/2004/13(09)/1468-06

Chinese Physics

© 2004 Chin. Phys. Soc.
and IOP Publishing Ltd

Optical properties and frequency conversion with $AgGaGeS_4$ crystal*

Ren De-Ming(任德明)[a], Huang Jin-Zhe(黄金哲)[a)b)†],
Qu Yan-Chen(曲彦臣)[a], Hu Xiao-Yong(胡孝勇)[a],
Andreev Yuri[c], Geiko Pavel[c], Badikov Valerii[d], and Shaiduko Anna[c]

[a] *Institute of Opto-Electronics, Harbin Institute of Technology, Harbin* 150001, *China*
[b] *Department of Applied Physics, Harbin University of Science and Technology, (West Campus), Harbin* 150080, *China*
[c] *Institute for Optical Monitoring, Siberian Branch, Russian Academy of Sciences, Tomsk* 634055, *Russia Federation*
[d] *Kuban State University, Krasnodar* 350040, *Russia Federation*

(Received 9 April 2003; revised manuscript received 13 May 2004)

The basic optical property and phase-matching of new mixed $AgGaGeS_4$ crystal are presented. Frequency conversion, in particular the SHG of 30ns pulses of 9μm emission band of transversely excited atmospheric-pressure (TEA) CO_2 laser, is realized in $AgGaGeS_4$ for the first time. As high as 0.57% peak power and 0.3% external energy efficiencies, and 0.7mJ harmonic pulse energy are obtained for the 9.55 μm emission line at pump intensity of 4% level of the damage threshold.

Keywords: $AgGaGeS_4$, nonlinear crystal, frequency conversion, second harmonic generation (SHG), CO_2 laser
PACC: 4270F, 4265K, 4255D

1. Introduction

Numerous nonlinear materials have been developed for different laser devices both for UV to near-IR and near-IR to mid-IR spectral ranges. Nowadays special interest is paid to frequency conversion of some laser sources in the near-IR and mid-IR ranges. These sources include solid state cw and long pulse Nd:YAG, holmium and erbium lasers, femtosecond Ti:sapphire, Nd:YAG and Cr:forsterite lasers, as well as Nd:YAG second harmonic and visible lasers. A special subject for concern is to design extra wide band 0.2–14μm laser source consisting of Nd:YAG laser and set of frequency converters or microchip lasers with specified frequency converters. Nd:YAG laser has high output power, so it is widely distributed and used in mobile systems. Frequency conversion of femtosecond lasers is, in its turn, the simplest way in design of middle IR tunable femtosecond sources. Spectroscopic parameters of middle IR emission generated by frequency conversion of visible range lasers can be controlled and adjusted with highly sensitive and well designed devices and media.

Unfortunately, at near-IR and visible spectral ranges, the most efficient mid-IR nonlinear crystals such as Te, $CdGeAs_2$ and Tl_3AsSe_3 are not transparent. From the near-IR to mid-IR, $ZnGeP_2$,$AgGaSe_2$, CdSe and GaSe with good optical quality now are available. However, due to large absorption at the band edge, the effective spectrum range of pump source for these crystals should be above 1μm. Though Ti:sapphire and Nd:YAG laser can be used as a pump source for $AgGaS_2$ [1] and $LiInS_2$ (d_{31}=6.2, d_{32}=5.4 and d_{33}=9.8pm/V),[2,3] which possess low figure of merit and birefringences and relatively low laser damage thresholds. That is why the design of high efficiency frequency converters of long duration laser pulses with these crystals is nearly impossible. The first direct frequency conversion of femtosecond lasers into the mid-IR with 1.5 mm length $LiInS_2$ by difference frequency generation (DFG) yielded only 2nJ in the 4.8–9.0μm range.[4] Because of low birefringence it is also impossible to realize the efficient up-conversion

*Project supported by National Natural Science Foundation of China (Grant No 69878005) and Natural Science Foundation of Heilongjiang province, China (Grant No F01-10).
†E-mail: huang_yin@sohu.com

of CO_2 laser into the visible range with $AgGaS_2$ and $LiInS_2$ according to the diagram 10.6+0.53→0.505μm or to generate mid-IR emission under any visible laser pump.

To avoid this difficulty attention has been directed to the modernizing of physical properties of well-known crystals by doping [GaSe:In], to find new and to develop mixed crystals. Recently, the crystal $CsGeCl_3$ [5] having wide infrared transmission coupled with visible transmission (0.4–20μm) has been reported. But this crystal is still in the development stage and also not commercially available. On the other hand, the solution of two chalcopyrite $A^IB^{III}C_2^{VI}$ crystals[6–9] or $A^{IV}B_2^{VI}$ in $A^IB^{III}C_2^{VI}$ [10] crystal is a prospective way to produce broad transparency and a high birefringence crystal. A mixed crystal has higher nonlinearity in comparison with a parent anisotropic crystal if the latter is isotropic or has low birefringence but higher nonlinearity. These crystals also possess 'noncritical phase-matching' (NCPM) for desired frequency conversion, by adjusting the mixing ratio x, broader transparency range, improved thermal properties and/or, in principle, higher damage threshold. Different laser devices employing NCPM have been reported with $CdGe(As_xP_{1-x})_2$ (mid-IR),[6] $AgGa_xIn_{1-x}Se_2$ (near- to mid-IR),[9,11–13] $AgGa_xIn_{1-x}S_2$,[8] $AgGa(S_xSe_{1-x})_2$ (long wavelength part of visible–mid-IR),[6,7] and $Cd_xHg_{1-x}Ga_2S_4$ (visible–mid-IR).[14] The new crystal $Nd:Ga_4RO(BO_3)_3$ (R=Gd,Y)[15] also has this property.

In this work, we continue the investigation of optical properties, phase-matching, damage threshold[10,14] and CO_2 laser SHG in mixed $AgGaGe_xS_{2(1+x)}$ crystal with a transparent range from the visible to mid-IR. In comparison with other efficient crystals in terms of physical properties and SHG efficiencies, $AgGaGe_xS_{2(1+x)}$ may be positioned importantly in frequency conversion, especially in relation to CO_2 laser SHG.

2. Optical properties

Silver germanium thiogallate crystal $AgGaGe_xS_{2(1+x)}$ is a kind of solid solution of anisotropic $AgGaS_2$ with low nonlinearity and isotropic GeS_2 with high nonlinearity. The chemical formulae are as follows:

(1) $AgGaS_2$:GeS_2 → $AgGaGe_xS_{2(1+x)}$, where x=1–9 is mixing ratio at 1103K;

(2) $AgGaS_2$:GeS_2 → $Ag_xGa_xGe_{1-x}S_2$, where x=0.17–0.54.

Though $AgGaGe_xS_{2(1+x)}$ was known in 1980 ($\phi 20\times 50 mm^2$ ingot was available[10]), detailed description of its optical properties and phase-matching was only published in 2002.[14] It belongs to the biaxial crystal class and to the mm^2 point group. It has a density of 3.80g/cm^3 and a melting temperature of 840°C which varies within a small temperature interval of 10K with x=1 to 9. Other data are listed in Table 1.

Table 1. Parameters of $AgGaGeS_4$ crystal.

$\Delta\lambda$/nm	Sellmeier coefficients				d_{ij}/(pm/V)	Lattice constant/nm
		X	Y	Z		a=0.685, b=1.205, c=2.295
4400–14000	A	12.644670	11.947671	11.143570		$X-b$, $Y-a$, $Z-c$
(0%)	B	–21966.269	–19915.432	–24267.167	$d_{31}=\pm 8.0$	At λ=1064nm: V_z=10.34°;
4450–11900	C	3000	3000	4000	$d_{32}=\pm 13.0$	n_x=2.342, n_y=2.341; n_z=2.287
(10%)	D	–0.17736979	–0.18261602	–0.16861483		λ=9550nm: V_z=12.5°;
	E	0.06821353	0.07099873	0.06081829		n_x=2.257, n_y=2.259, n_z=2.222

Here $\Delta\lambda$ is the transparency spectral range at zero (0%) and ten percent (10%) levels; X, Y, Z and d_{ij} are optical axes and second-order nonlinear susceptibility coefficients respectively; a, b and c are lattice parameters, V_z is angle between Z and optical axis. Sellmeier equations are in the form $n^2 = A + B/(C\text{-}\lambda^2) + D/(E\text{-}\lambda)^2$ and n_x, n_y, and n_z are principle refraction indices estimated at 0.45 to 11.5μm wavelength. It is noteworthy that relations X, Y, Z → b, a, c and $n_x > n_y > n_z$ at short wavelengths range are accepted. The order relation between n_x and n_y depends on wavelength. For example, $n_x < n_y$ holds at CO_2 laser wavelengths, while at 7.565μm it becomes $n_y = n_x$ which implies the characteristic of a uniaxial crystal. At the maximal transparency range birefringence is $B \approx 0.057$ ($B = n_s - n_f$, s, f→ slow, fast respectively) which is higher than that ($B \leq 0.053$) of parent anisotropic $AgGaS_2$ crystal within $\pm 2.5\times 10^{-4}$ measurement accuracy of refractive indices. Lattice parameters a, b, and c will change into a=6.88, b=11.85,

c=22.66 (×0.1nm) with x approaching to 9 from number 1.

In this work yellowish $10\times15\times2.1\text{mm}^3$ sized $AgGaGeS_4$ crystal which is cut at θ=59°54′±10′ (from Z axis) for type I SHG in the YZ plane is used. It was grown by the Bridgman–Stockbarger method with 14mm/day speed at 6°C/mm temperature gradient. The optical transparency range of this crystal is shown in Fig.1.

The short wavelength transmission is measured with a Shimadzu UV-3101PC spectrophotometer supplied with polarizer and ϕ2mm diaphragm and the mid-IR transmission is measured with a Specord 80M in local regions as shown in Fig.1. The transparency range is 0.44–14.0 and 0.445–11.5μm at '0' and 10% level, respectively. The specific absorption peaks found in the transparency spectrum of mixed $AgGa_{1-x}In_xSe_2$[13] and $Cd_xHg_{1-x}Ga_2S_4$[14] crystals are absent here. At maximal transparency range, the coefficient of optical extinction is $\alpha \leq 0.2\text{cm}^{-1}$ and transparency variations are within 1–2%. At CO_2 laser wavelength, the extinction coefficient resulting from low intensity phonon absorption is less than 0.3cm^{-1}, which is lower than the values of high quality $ZnGeP_2$ (α=0.27–1.0cm^{-1}) and $LiInS_2$ (α=1.1–2.3cm^{-1}). The transparency spectrum is also not dependent on the polarization of the incident beam and its uniformity is in coincidence with the results of chemical microanalysis by the e-beam microscope of M/S Joel, Japan, supplied with spectrophotometric attachment (Link, Germany). Maximal variations of the crystal component from region to region are as follows: $Ag_{1\pm0.019}Ga_{1\pm0.021}Ge_{1\pm0.012}S_{4\pm0.004}$ at local area of $1.2\times1\text{mm}^2$ with a depth of 500nm. So, within experimental error, crystal composition is uniform and stoichiometric. However, the $AgGaGeS_4$ crystal has visual nonuniformity formed by usual internal swells. For the first time, the short wavelength absorption shoulder at 0.44–0.9μm has been observed clearly at specially chosen local regions as shown by points 1–6 in Fig.1. The maximal extinction is α=0.2–0.3cm^{-1} at 0.5μm.

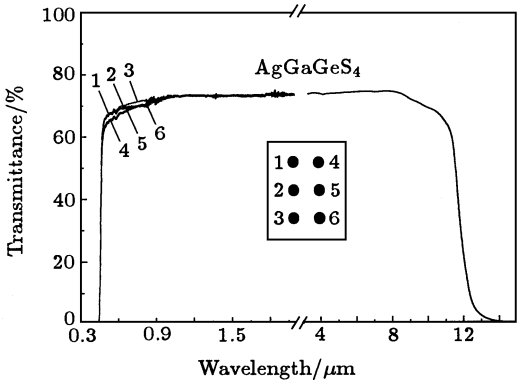


Fig.1. Transparency spectrum of 2.1mm thick $AgGaGeS_4$ at six local regions in accordance with internal map.

3. Phase-matching

Possible nonlinear processes in $AgGaGeS_4$ crystal are $ee-o$ in the XY plane, $oo-e$ in the YZ and XZ planes at $\theta < V_z$, and $oo-e$ in the XZ plane at $\theta > V_z$ respectively. The transitions between stereographic projections of phase-matching directions for SHG estimated in the common case over the spectral range 0.45–11.5μm is represented in Table 2.

Table 2. The transitions between stereographic projections of phase-matching directions for SHG.

Type	00	00–10	10	10–30	30	30–31	31	31–33	33	33–31	31	31–30	30	30–10	10	10–00	00
^{s}ff	1318.8					2161.7		2216.1		8384.5		8446.8					11000
^{ss}f	1318.8	1536.8		1536.7										10586		10897	11000

Here X is the horizontal axis and Z is the vertical axis and the Y axis is orthogonal to projections. Transition wavelengths from one to other type projections are listed in the second line of Table 2. Solid line denotes Type I phase-matching, while dotted line denotes Type II. It can be seen that SHG can be realized in a wide spectral range from 1.537 to 10.9μm. SHG phase-matching takes place in all three main planes: XY, YZ, and XZ. Type I $oo \rightarrow e$ phase-matching at CO_2 laser wavelengths exists in both the YZ plane with θ=62°42′ and the XZ plane with θ=60°12′ but with 37° and 25° respectively at CO laser wavelengths. The SHG phase-matching diagram in the YZ plane is presented in Fig.2(a).

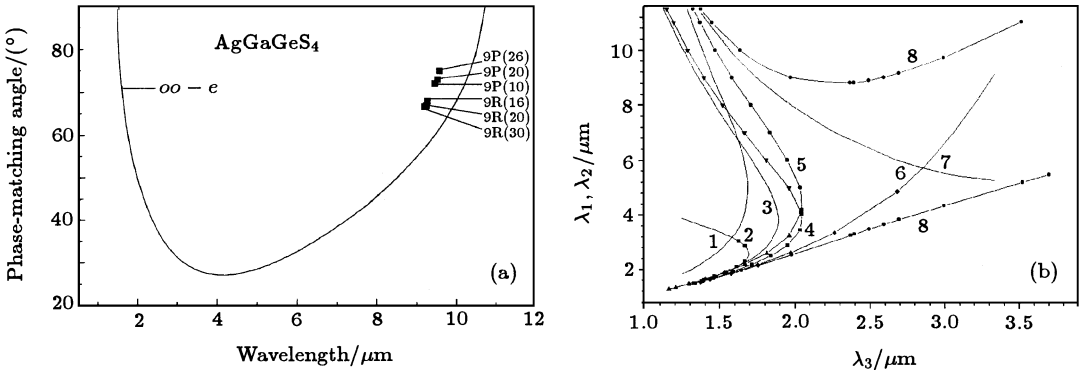


Fig.2. SHG phase-matching diagram in the YZ plane, where the points are experimental data (a); group-velocity matching diagrams in YZ plane in the form of s_1-f_3(1) and f_2-f_3(7) as sff-type; s_1-s_2(3), s_1-f_3(4), s_2-f_3(5) as ssf- and s_2-f_3(2), f_1-f_3(6), and f_1-s_2(8) as fsf-type (b).

The spectral and internal angular bandwidths of SHG in YZ plane versus wavelength are shown in Fig.3. Both bandwidths are noncritical and attractive for practical application. Large birefringence permits realizations of 1.1–11.5μm 'optical parametric oscillator' (OPO) pumped by Nd:YAG laser and 4.0–11.5μm OPO pumped by Cu:vapour laser, as well as up-conversion of CO_2 laser emission by mixing with 0.505μm emission of Cu:vapour laser.

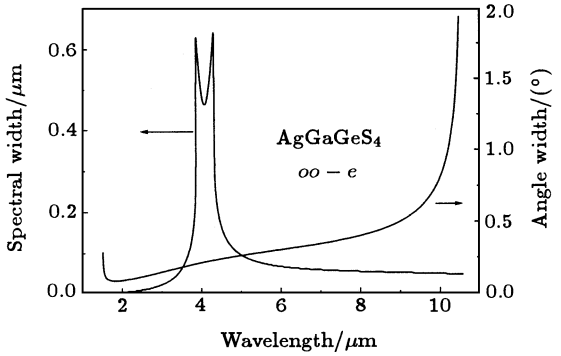


Fig.3. Spectral and angular bandwidths of SHG in YZ plane versus wavelength.

It is well known that in comparison with uniaxial crystals, biaxial ones present much larger possibilities of phase-matching. Moreover, biaxial crystals are very promising for frequency conversion of a femtosecond laser since it is easy to find group-velocity matching simultaneously satisfying common phase-matching. Group-velocity matching in the phase-matching direction for three wave interactions in the YZ plane is represented in Fig.2(b), where ssf is type I phase-matching, fsf is type II and sff is type III. The curves labelled as '1' to '8' in Fig.2(b) stand for group-velocity matching in the three types of phase-matching ssf, fsf, sff. As can be seen from Figs.2 and 3, $AgGaGeS_4$ is suitable for 'optical parametric generation'(OPG) of mid-IR femtosecond pulses, under direct pump by a femtosecond Cr:forsterite laser. It is known that increasing the mixing ratio leads to a shift of refractive indices and birefringence that opens additional potential in long pulse and femtosecond laser frequency conversion. For instance, by changing the mixing ratio x from 1 to 5, the birefringence of mixed crystal is doubled.[9]

4. Experiment and discussions

The damage threshold of $AgGaGeS_4$ is redetermined with a homemade TEA CO_2 laser in comparison with a number of known and new crystals which are of similar optical quality at the maximal transparency range and at identical experimental conditions. A modernized version of the measurement procedure and equipment described elsewhere[16] is used in this case. An integrating sphere is installed before a calibrated Au:Ge photoresistor to increase measurement accuracy. The laser in 9P(20) emission line (9.55μm), operating in TEM_{00} mode, emits over a half of Joule 30±1 ns (FWHM) pulse, consisting of a leading peak with about 90% of total energy and low intensity 'tail'. The energy variations of the total pulse and leading peak do not exceed 3.5% and 2% respectively. All tested crystals are cut for SHG at 9μm band of CO_2 laser emission. Measurements show that the damage threshold of $AgGaGeS_4$ is 230 MW/cm^2, which is 1.5 to 1.7 times higher than that of $CdGeAs_2$ (157 MW/cm^2), $ZnGeP_2$(142), $AgGaSe_2$ (139), and $AgGaS_2$ (149) but 25% lower than that of $HgGa_2S_4$(310).

The known data on optical properties and damage thresholds permit estimation of the potential efficiency of $AgGaGeS_4$ in frequency conversion. We summarize its SHG efficiency in Table 3 together with other mid-IR crystals.

Table 3. Potential efficiencies of CO_2 laser SHG in mid-IR crystals.

Crystal	$\Delta\lambda$/nm	$n_{9.55}$	B	d_{ij}/(pm/V)	$d_{\rm eff}$/(pm/V)	P/(°)	$M_{\rm sh}$/(pm/V)^2	M'/%	$I_{\rm d}$/arb.units	$M_{\rm sh}\times I_{\rm d}$/%
$ZnGeP_2$	700–12000	3.10	0.04	d_{36}=75	$d_{36}\sin 2\theta$	68.6	87.2	100	1	1
$AgGaS_2$	470–10000	2.36	0.053	d_{36}=11.7	$d_{36}\sin\theta$	58	7.5	8.6	1.05	9
$AgGaGeS_4$	450–14500	2.259	0.057	d_{32}=13	$d_{32}\sin^2\varphi + d_{31}\cos^2\varphi$ (XY)	–	–	–	1.6	–
		2.257		d_{31}=8	$d_{32}\sin\theta$ (YZ)	61.5	11.8	13.5		21.6
		2.222			$d_{31}\sin\theta$ (XZ)	56.5	3.2	3.7		5.9
$LiInS_2$	450–15000	2.129	0.053	d_{31}=6.2	$d_{31}\cos^2\varphi + d_{32}\sin^2\varphi$ (XY)	63	8.7	10	1.3	13
(CO laser)		2.165		d_{32}=5.4	$d_{32}\sin\theta$ (YZ)	–	–	–		–
		2.173			$d_{31}\sin\theta$ (XZ)	40.5	4.1	4.7		6.1

Here $\Delta\lambda$ is the transparency range at '0' level, $n_{9.55}$ is average, meaning of refraction index at 9.55μm, B is the maximal birefringence, d_{ij} and $d_{\rm eff}$ are the second-order nonlinear susceptibility coefficient and the effect coefficient respectively, P is phase-matching angle, $M_{\rm sh}$ and M' are absolute and normalized figure of merit for SHG, and $I_{\rm d}$ is damage threshold. The relation $n_x < n_y \leq n_z$ is accepted for $LiInS_2$, which is the only available crystal suitable for direct frequency conversion of femtosecond lasers in the mid-IR range.[17] Processes $oe-e$ and $eo-e$ exist in $LiInS_2$ in the XY plane, $oe-o$ and $eo-o$ in the YZ, and $oo-e$ in the XZ plane respectively. Unfortunately, $LiInS_2$ does not show phase-matching for the SHG of the phase-matching CO_2 laser. To compare the potential efficiencies of $AgGaGeS_4$ and $LiInS_2$, we list related data of the two crystals on SHG of CO laser (5.3μm) in Table 3. It should be noted that the nonzero nonlinear susceptibility coefficient d_{33} cannot be utilized in frequency conversion for both $AgGaGeS_4$ and $LiInS_2$ crystals, and the relative sign of d_{31} and d_{32} in $AgGaGeS_4$ is still undetermined but taken as positive in estimation.

The SHG is performed at 9μm emission band of the CO_2 laser at different local regions of $AgGaGeS_4$. In experiment, the laser pulse, with ϕ5mm waist and 33±1ns duration, possesses total energy up to 240±0.2mJ with energy density 1.22±0.01 J/cm^2, which accounts for peak power 7.6±0.8MW and peak intensity 38.5±0.4MW/cm^2 respectively. The pulse energy is monitored by an IMO-2N calorimeter but the wave shape is recorded by a Ge drug detector (Δf =1GHz) which is connected to a TDS-210 oscilloscope (Δf=60MHz, a sampling time of 1ns) and to PC through an analogue–digital convertor (ADC). The measured energy values and the stored oscilloscope traces of the pulse shape are combined to determine the mean energy and root-mean-square (RMS) deviations of the total energy and peak power. The final result is statistically averaged on 10 data each. Doubled surfaces of refraction indices of $AgGaGeS_4$ and their orientation are illustrated by the first octant in Fig.4(a); SH energy of the TEA CO_2 laser in 9.55μm emission line versus mismatch angle, as well as SH energy versus wavelength, are shown in Figs.4(b) and 4(c) respectively.

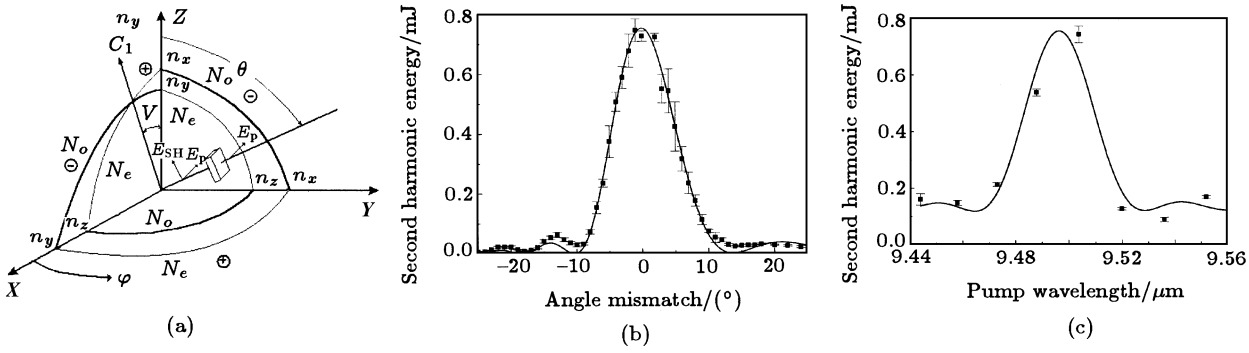


Fig.4. Doubled surface of refraction indices of $AgGaGeS_4$ crystal (a). Here C_1 is optical axis, $N_{\rm o}$ and $N_{\rm e}$ are refraction indices for o- and e- waves; n_x, n_y, n_z are refraction indices in the direction of x, y, z axes, '⊕' and '⊖' are sectors in the limit of which the crystal is positive and negative, V is the angle between optical and Z axes, ϕ and θ are phase-matching angles in the XY and YZ planes, and $E_{\rm p}$ and $E_{\rm sh}$ are pump and second harmonic polarization direction. SHG energy of 9.55μm emission line versus mismatch angle (b) and wavelength (c).

The experimental phase-matching angles are about 10° higher than the estimated ones (in Fig.2(a)). In the 9P(20) emission line (9.55μm), for example, it is $72°54' \pm 5'$ and just 10° offset from estimation. About 43.04±0.21kW peak power and 0.57±0.07% external peak power, conversion efficiency of SHG is obtained under pump of 38.5±0.4MW/cm^2. The pump intensity is only 4% of its damage threshold. Such a low intensity excludes the influence of self-heating on measurement results. On this condition external energy conversion efficiency is 0.30±0.04% and SH energy is 0.7±0.1 mJ. To our knowledge, this is the first time that frequency conversion in $AgGaGeS_4$ has been realized. It is also developed that the ratio of SHG efficiencies between $AgGaGeS_4$ and $ZnGeP_2$($10\times10\times4$mm^3 sample) is about 1/5, in accurate coincidence with the estimation presented in Table 3 for identical thickness (normalized) $ZnGeP_2$ and $AgGaGeS_4$.

5. Conclusion

Linear and nonlinear optical properties of mixed $AgGaGeS_4$ crystal ($AgGaS_2$:GeS_2 or $AgGaGe_xS_{2(1+x)}$ at mixing ratio x=1) have been investigated in detail. Mixing of anisotropic $AgGaS_2$ and isotropic GeS_2 crystals reveals not only expansion of transparency range and increment of birefringence but also obvious promotion of the damage threshold. Frequency conversion, i.e. SHG in TEA CO_2 laser, is realized for the first time in $AgGaGeS_4$ crystal with an efficiency of 0.57% of peak power and 0.3% of external energy, where pumping intensity is as low as 4% of its damage threshold. The measured SHG efficiency and phase-matching angles are in good coincidence with the estimation. The SHG efficiency of $AgGaGeS_4$ pumping by CO_2 laser is about 20% of the value of the middle IR crystal $ZnGeP_2$ but 2.4 times the efficiency of $AgGaS_2$. Its birefringence is large enough to provide 1.1–11.5μm OPO pumped by Nd:YAG laser and 4.0–11.5μm OPO pumped by Cu:vapour laser, as well as up-conversion of CO_2 laser by mixing with 0.505μm emission of Cu:vapour laser. $AgGaGeS_4$ crystal along with its mixing family of $AgGaGe_xS_{2(1+x)}$ may have twice or even higher potential efficiency in direct frequency conversion of available femtosecond lasers into the mid-IR range compared with the available crystal $LiInS_2$.

References

[1] Gurzadyan G G, Dmitriev V G and Nikogosyan D N 1999 *Handbook on Nonlinear Optical Crystals* (Berlin: Springer) p132

[2] Huang J Z, Ren D M, Hu X Y, Qu Y C, Andreev Y, Geiko P, Shaiduko A and Grechin S 2003 *Chin. Opt. Lett.* **1** 237

[3] Isaenko L, Vasilieva I, Yelisseyev A, Lobanov S, Malakhov V, Dovlitova L, Zondy J J and Kavin I 2000 *J. Cryst. Growth* **218** 318

[4] Rotermund F, Petrov V and Noak F 2001 *Appl. Phys. Lett.* **78** 2623

[5] Gu Q T, Fang C S, Shi W, Wu X W and Pan Q W 2001 *J. Cryst. Growth* **225** 501

[6] Mikkelson J C and Kildal H 1978 *J. Appl. Phys.* **49** 426

[7] Cheng G C, Yang L, Wu H X and Cheng N 1995 *Acta Opt. Sin.* **15** 375 (in Chinese)

[8] Badikov V V, Matveev I N, Panyutin V B, Pshenichikov S M, Rozenson A E, Skrebena S V, Trotsenko N K and Ustinov N D 1980 *Sov. J. Quantum Electron.* **7** 2237

[9] Bhar G C, Das S, Chatterjee U, Datta P K and Yu M Andreev 1993 *Appl. Phys. Lett.* **63** 1316

[10] Badikov V V, Tyulyupa A G, Shevyrdyaeva G S and Sheina S G 1991 *Inorg. Mater.* **27** 248 (in Russian)

[11] Schunemann P, Setzler S and Pollock T M 2000 *J. Cryst. Growth* **211** 257

[12] Takaoka E and Kato K 1999 *Opt. Lett.* **24** 903

[13] Andreev Yu M, Baturin I S, Geiko P P and Gusamov A I 1999 *Quantum Electron.* **29** 904

[14] Andreev Yu M, Badikov V V, Geiko L G, Geiko P P and Grechin S G 2002 *Appl. Phys. J.* **2** 102 (in Russian)

[15] Wang Z P, Xu X G, Sun X, Fu K, Song R B and Shao Z S 2002 *Acta Phys. Sin.* **51** 2029 (in Chinese)

[16] Andreev Yu M, Badikov V V, Voevodin V G, Geiko L G, Geiko P P, Ivashchenko M V, Karapuzikov A I and Sherstov I V 2001 *Quantum Electron.* **31** 1075

[17] Andreev Yu M, Geiko L G, Geiko P P and Grechin C G 2002 *Conf. Atomic and Molecular Pulsed Lasers AMPL-2001, Proc. SPIE* **4747** 400